^{13}C NMR studies of conformational dynamics in 2,2,5,7,8-pentamethylchroman-6-ol derivatives in solution and the solid state

Stanislaw Witkowski,*[a] Dorota Maciejewska[b] and Iwona Wawer[b]

[a] *University of Bialystok, Institute of Chemistry, Pilsudskiego 11/4, 15-443 Bialystok, Poland*
[b] *Medical University of Warsaw, Faculty of Pharmacy, Department of Physical Chemistry, Banacha 1, 02-097 Warsaw, Poland*

Received (in Cambridge, UK) 23rd February 2000, Accepted 12th May 2000
Published on the Web 12th June 2000

Conformational preferences of esters of 2,2,5,7,8-pentamethylchroman-6-ol were studied by means of dynamic ^{13}C NMR in solution and the CP MAS technique in the solid phase. An increase in the rigidity of ester molecules in comparison with free chroman-6-ol was observed. The coalescence of the signals of the *gem*-dimethyl group was monitored and discussed in terms of hindered rotation around the C–O_{ester} bond; the dynamic parameters (k, $\Delta G^{\ddagger}$) were determined. The barrier is determined by the interplay of steric and electronic effects of substituents in the ester fragment. GIAO-CPHF MO calculations of shielding constants were performed for the conformations with the carbonyl group of the ester substituent located below and above the plane of the aromatic ring.

Introduction

α-Tocopherol is not only the most biologically active component of vitamin E but is also one of the best chain-breaking phenolic antioxidants known. There is now general agreement that it functions as a free radical scavenger *in vivo*, particularly in intracellular membranous organs where most of the vitamin is distributed.[1,2]

2,2,5,7,8-Pentamethylchroman-6-ol (**1**) is often used as a

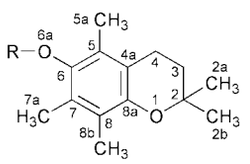

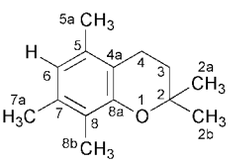

11

1: R = H
2: R = acetyl
3: R = propionyl
4: R = trifluoroacetyl
5: R = trichloroacetyl
6: R = pivaloyl
7: R = ethoxycarbonyl
8: R = benzoyl
9: R = nicotinoyl
10: R = tosyl

model compound for studies of structural and physicochemical aspects of α-tocopherol (vitamin E) biological activity. Due to the lack of a lipophilic phytyl side chain, compound **1** does not show any vitamin E activity, because it cannot be incorporated into phospholipid bilayers.[2] Nevertheless chromanol **1** is convenient for investigation of stereoelectronic and conformational effects in the chromane system.[3] X-Ray analysis of crystalline **1** showed two structurally different molecules in the unit cell (the main difference is that torsional angles between O1–C2 and the aromatic ring are 15.3° and 18.5°, respectively).[4,5] According to the Cambridge Structural Data Base and our knowledge there are no XDR data on esters of chromanol **1**. In the crystal state the heterocyclic ring adopted a half chair conformation, and in solution two interconverting conformers of the flexible semi-unsaturated chromane ring in approximately equal populations were suggested.[4,6]

The aim of this work is to provide more information about the molecular dynamic and conformational preferences of 2,2,5,7,8-pentamethylchroman-6-ol derivatives: esters (**2**–**10**) and 2,2,5,7,8-pentamethylchromane (**11**). Steric hindrance of the flanking methyl groups (C5a and C7a) to the rotation of an ester residue around the benzene-to-oxygen bond probably influences conformational preferences in the chromane system.[7] For a quantitative estimation of this effect in molecules, dynamic ^{13}C NMR was used. In order to obtain chemical shifts for solid compounds the ^{13}C CP MAS NMR spectra were also recorded.

Results and discussion

Dynamic NMR investigation

^{13}C NMR spectra of compounds **1**–**11** were measured for $CDCl_3$ solutions. Chemical shifts are collected in Table 1. The ^{13}C spectra of compounds **2**–**10**, measured at room temperature, showed that the signal at *ca.* 27 ppm, ascribed to C2a and C2b of the *gem*-methyl groups, was markedly broadened in acetate **2**, propionate **3** and trichloroacetate **5**. In pivaloate **6**, benzoate **8** and nicotinate **9** these groups gave two completely separated singlets at ambient temperature. Surprisingly, no similar effect in free phenol **1** and in the 6-deoxy-α-model **11** was observed. One can conclude that esterification of the 6-OH group causes an increase in rigidity of these molecules, in comparison with the parent chroman-6-ol **1**. In order to establish kinetic parameters for the observed dynamic process, the ^{13}C NMR spectra of compounds **1**–**5**, **7**, **10** and **11** were recorded in the temperature range −60 °C to +50 °C (213–333 K). At lower temperatures, separation of signals for C2a and C2b was achieved for **2**–**5**, **7** and **10**. The spectra of acetate **2** in the range 25–28 ppm at low temperatures are presented in Fig. 1, as an illustration. The spectra recorded for propionate **3** at 213 K showed that the difference in the ^{13}C chemical shift of C2a and C2b is 1.2 ppm, decreases to 0.86 ppm at 243 K and further to 0.62 ppm at 283 K. In order to determine life-times, line shape analysis of broadened signals near the coalescence point (using a computer program for two-site exchange A ⟷ B[8]) was carried out. Convergent results were found on iteration with life-times τ, transverse relaxation times T_{2A} and T_{2B} and site frequencies ν_A, ν_B. The initial values of T_{2A} and T_{2B} for iteration were obtained from the measured line width of the nearby C3 and C4 carbon resonance lines. The kinetic parameters are collected in Table 2.

Table 1 Chemical shifts of compounds **1**–**11** for ^{13}C NMR in $CDCl_3$ solutions and CP MAS (acyl residue signals were omitted)

Compound		C2	C2a	C2b	C3	C4	C4a	C5	C5a	C6	C7	C7a	C8	C8a	C8b	Ester C=O
1	293 K	72.37	26.60	26.60	32.97	20.99	117.00	118.65	11.17	144.49	121.17	12.11	122.43	145.61	11.70	—
	MAS	72.8	31.0	22.9	32.4	21.5	117.1/	120.5	11.6	142.6	121.6	11.6	123.3/	146.2	11.6	—
			(−4.4)	(+3.7)		(−1.5)	115.0	(−1.9)		(+1.9)			124.5			
2	293 K	72.90	26.86	26.86	32.60	20.84	117.07	122.91	11.76	140.50	124.84	12.88	126.60	149.44	12.02	169.64
	273 K		27.21	26.48												
	MAS	73.7	29.2	23.7	33.3	21.9	117.5	122.6	11.4	144.7	126.2	11.4	127.0	148.8	11.4	168.3
			(−2.3)	(+3.2)						(−3.9)						(+1.3)
3	293 K	72.90	26.79	26.79	32.65	20.87	117.09	122.91	9.43	140.48	124.88	12.95	126.55	149.37	12.00	172.96
	213 K	72.97	27.20	26.00	31.97	20.71	117.13	122.77	9.56	139.59	124.90	13.02	126.43	148.98	12.21	
	MAS	73.1	31.4	25.6	33.5	20.7	118.8	122.2	10.1	141.4	126.3	13.4	127.0	148.6	11.6	172.0
			(−3.4)	(+1.2)			(−1.7)									(+1.0)
4	293 K	73.33	26.73	26.73	32.48	20.84	117.68	123.71	11.68	139.36	124.35	12.50	125.96	150.43	11.78	155.54
	253 K	73.34	27.28	26.63	32.50	21.03	117.71	123.72	11.71	139.36	124.36	12.54	125.98	150.42	11.81	
	MAS	73.7	30.1	23.3	32.9	19.9	118.8	124.3	10.1	139.3	125.2	11.8	125.2	150.3	11.8	155.5
			(−3.7)	(+3.4)												
5	293 K	73.23	26.74	26.74	32.51	20.82	117.56	123.55	11.75	140.47	124.67	12.58	126.36	150.22	11.78	160.51
6	293 K	72.87	26.99	26.41	32.72	20.89	117.11	122.91	11.74	140.55	124.87	12.70	126.70	149.26	11.85	185.36
	MAS	72.6	30.7	23.1	31.5	21.4	117.5	123.7	11.6	140.6	125.8	12.5	127.5	148.1	11.6	174.6
			(−3.7)	(+3.3)												(+10.8)
7	293 K	72.85	26.68	26.68	32.56	20.73	117.02	122.88	11.63	140.91	124.94	12.51	126.70	149.45	12.18	153.76
8	293 K	72.99	27.05	26.58	32.69	20.92	117.25	123.08	11.84	140.66	123.08	13.02	126.90	149.53	12.18	172.39
9	293 K	72.87	26.91	26.46	32.72	20.89	117.11	122.91	11.74	140.58	124.87	11.94	126.70	149.26	12.70	163.51
	MAS	73.4	30.0	22.3	32.4	22.3	117.1	122.9	12.3	140.5	125.9	12.3	127.0	149.2	12.3	163.2
			(−3.1)	(+4.2)												
10	293 K	73.27	26.77	26.77	32.56	20.92	117.70	123.52	11.87	140.16	123.52	14.23	127.46	150.01	13.50	—
11	293 K	72.87	26.78	26.78	32.65	20.34	116.45	122.18	14.11	134.48	121.84	19.66	133.21	151.66	18.72	—

The rate constants obtained at several temperatures were used for the determination of free energies of activation. The values of $\Delta G^{\ddagger}$ for the coalescence temperature have been taken as a measure of a barrier. The range of $\Delta G^{\ddagger}$ is from 63.5 kJ mol^{-1} for pivaloate **6** to *ca*. 41.8 kJ mol^{-1} for tosylate **10**. In the spectra of tosylate **10** the common signal of 2a and 2b methyl groups became broader with decreasing temperature. At 208 K the coalescence temperature was almost achieved. The separation of carbon resonances was not obtained for $CDCl_3$ solutions; therefore the case could not be treated quantitatively. The rate constant was calculated assuming the same differences in chemical shifts as those observed for other compounds. It is worth noticing that a barrier for chroman-6-ol **1** is significantly lower. No broadening of 2a and 2b methyl signals in **1** even at 208 K was observed. Assuming a life-time of the order 0.002 s at 208 K, the barrier can be estimated as <34 kJ mol^{-1}.

All esters **2**–**10** exhibit a higher barrier than the parent chroman-6-ol **1**. Comparing the values of $\Delta G^{\ddagger}$ for esters, the following sequence of $\Delta G^{\ddagger}$ has been determined: pivaloate **6** > benzoate **8** > nicotinate **9** > acetate **2** > propionate **3** > trichloroacetate **5** > trifluoroacetate **4** > ethyl carbonate **7** > tosylate **10**. It is worth noting that the lowest barriers were observed for derivatives **7** and **10**, where acyl groups were not standard (ethoxycarbonyl and tosyl, respectively). The ester groups listed above are of various sizes and types and their influence on the chroman-6-ol system results from combined steric and electronic effects.

There was a controversy regarding the assignment of the dynamic process observed in this type of compound, *i.e.* whether the observed dynamic process was caused by hindered rotation about the C_{Ar}–O bond or by heterocyclic ring inversion (by pseudorotation). In *gem*-disubstituted cyclohexanes the barrier to ring flipping is 40–45 kJ mol^{-1}. Cyclohexene assumes a more flattened conformation and the barrier to ring inversion is lower; the free energy of activation for 4,4-dimethylcyclohexene-d_4 is 25.5 kJ mol^{-1} (coalescence temperature −155.8 °C).[9] In the compounds with ring oxygen the C–O bonds are shorter than the C–C ones (energy for pseudorotation increases) and the steric hindrance in the transition state of inversion should be reduced (absence of two hydrogens). The contribution of these two effects is difficult to estimate, however, tetrahydropyran exhibits a barrier to ring inversion of 42.1 kJ mol^{-1},[10] similar to that of cyclohexane. It is probable, therefore, that $\Delta G^{\ddagger}$ for the semi-unsaturated ring inversion is only 25–30 kJ mol^{-1}, and that the dynamic process showing a higher barrier (of 41.8–63.5 kJ mol^{-1}, as observed by us in **2**–**10**) results from hindered rotation of the ester group at C6.

The barrier of 46 kJ mol^{-1} was determined[7] for hindered rotation around the benzene-to-oxygen bond in the esters of phenol that contained methyl substituents in both *ortho* positions; at −60 °C each of these methyl groups gave a separate signal. The authors believed that *cis–trans* isomerism or slow rotation around the carbonyl-to-oxygen bond is unlikely. According to Siddal *et al*.[7] the stiffness in the carbonyl-to-oxygen bond would increase the steric interference in the rotational excited state, which is approximately coplanar. Thereby the excited state is destabilised and slow rotation around the benzene-to-oxygen bond occurred.

However, a plot of $\Delta G^{\ddagger}$ values (Table 2) against van der Waals volumes (as well as van der Waals radii) of the substituents R in **2**–**10** does not form a continuous curve. It is scattered and the expected trend of increasing $\Delta G^{\ddagger}$ with increasing bulkiness was not observed, even without **7** and **10**, as illustrated in Fig. 2.

Voluminous substituents (pivaloate, benzoate and nicotinate) exhibit high rotational barriers, however for the small ones like acetate or trifluoroacetate the correlation is not valid. It is clear that for compounds **2**–**6**, **8** and **9** steric requirements of the O–(C=O)– fragment are similar and, therefore, electronic effects of a group linked to carbonyl should be more important. These effects are transmitted through the carbonyl carbon and O6 oxygen and determine the character of the C–O6a, O6a–C6 bonds.

Theoretical MO calculations

The barriers to heterocyclic ring inversion and hydroxy group rotation around the C6–O bond in α-tocopherol and chroman-6-ol **1** were studied theoretically by molecular mechanics MMP2, semi-empirical MNDOC[11] and Monte Carlo methods.[12] The calculated barrier for pseudorotation in the semi-unsaturated ring of chroman-6-ol **1** amounted to 5.9 kJ mol^{-1}; it is reduced by 1.3 kJ mol^{-1} due to the presence of the

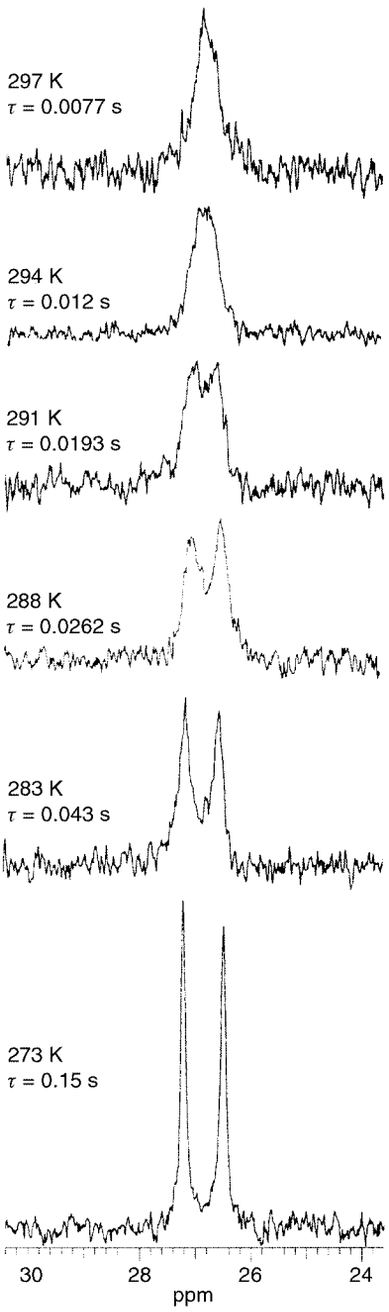

Fig. 1 The 2a and 2b methyl carbons of **2** in the temperature range 253–297 K.

aromatic ring (as compared with 7.2 kJ mol^{-1} for 2,2-dimethyl-3,4-dihydro-2*H*-pyran [12]). The neighbouring methyl groups (5a, 7a) do not influence the energy of ring inversion in chroman-6-ol. The isolated tocopherol molecule exhibits two half chair conformations of the semi-unsaturated ring and two energetically equivalent OH group conformations (twist angle ±90°), separated by an extremely low barrier.[11] This degeneracy disappears in the complex with fatty acids;[12] the α-orientation of the OH group, α-phytyl chain and β-axial C2-methyl is preferred.

In order to estimate conformational preferences of chroman-6-ol derivatives and the effect exerted by the ester groups, some theoretical calculations were performed. The semi-empirical PM3 method was chosen because it gives an improvement in treating relatively large molecules containing oxygen.[13–15] The geometry of **2**–**6** was optimised with respect to all parameters. The optimised structures were used for further *ab initio* calculations with the 6-31G** basis set. The calculations of the ^{13}C, ^{1}H and ^{17}O shielding constants were performed with the use

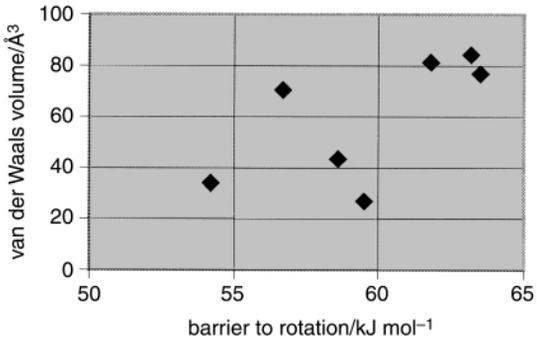

Fig. 2 The plot of $\Delta G^{\ddagger}$ (kJ mol^{-1}) *vs.* van der Waals volumes (Å^3).

of the GIAO-CHF method [16] for the structurally related compounds acetate **2**, trifluoroacetate **4**, trichloroacetate **5** and pivaloate **6** (Table 3).

The replacement of the –C(CH$_3$)$_3$ group by –CH$_3$ and further by –CCl$_3$ and –CF$_3$ in the ester fragment produces a subsequent decrease in the barrier (Table 2) and a redistribution of electron density, mainly within the –(C=O)–O6a–C6 fragment. A remarkable increase of shielding takes place for the carbonyl carbon (σ changes from 29.3 in **2** to 40.3 in **4**, Table 3; the observed values of δ are from 185.4 in **6** to 155.5 in **4**, Table 1). A deshielding of carbons *ortho* (C5 and C7) and *para* (C8a) and an increase in shielding of the *ipso* carbon (C6) could be expected, taking into account increasing electron acceptor properties of the substituents. Inspection of the respective chemical shifts (Table 1) confirms the above predictions. Indeed, such effects are observed and are well reproduced by calculations (Table 3). The influence of remote substituents reaches the ring oxygen: in the order **6**→**2**→**5**→**4** there is a tendency towards deshielding of O1 and its neighbour carbons C8a and C2.

Frozen rotation around the C6–O6a bond led to the differentiation of the α (downward, *i.e.* C=O below the plane of the aromatic ring) and β (upward) sides of the molecule, as illustrated in Fig. 3.

The calculations were carried out for both orientations. There is no significant energetic preference for any of these locations since the differences in heats of formation are less than 1 kJ mol^{-1}. The distance between the β axial methyl carbon (C2b) and the β carbonyl oxygen is 6.8 Å (α carbonyl, 8.3 Å). The orientation of the ester group does not affect the shielding of C2a (equatorial CH$_3$) whereas the changes of shielding of C2b (axial) are within ±0.2 ppm. The differences in chemical shifts between C2a and C2b are 5.5–8.1 ppm in the solid state, in agreement with the calculated values of shielding (σ). Only 0.6–1.2 ppm separations of methyl signals were observed at low temperature in solution spectra, indicating that the averaging of axial and equatorial orientations still proceeds (ring inversions). The differences in shielding (α or β location of ester C=O group) calculated for methyl carbons C5a and C7a are 0.1–1.0 ppm, however no doublet signals (as in ref. 10) were observed at low temperature when the rotation of the ester fragment was frozen.

If we compare the structures **6**, **2**, **5** and **4**, containing ester groups (CH$_3$)$_3$CCOO, CH$_3$COO, CCl$_3$COO and CF$_3$COO, respectively, one can see that the C6–O6a bond becomes longer, whereas the C–O6a and C=O bonds become slightly shorter, in agreement with the decreasing barrier to rotation around C6–O6a. The relationship between the carbon–oxygen bond lengths (from PM3 calculations) for C=O, O6a–C, O6a–C6, O1–C8a and O1–C2 and $\Delta G^{\ddagger}$ values for compounds **6**, **2**, **5** and **4** is presented in Fig. 4.

Solid state NMR

^{13}C NMR spectra for solid compounds **1**–**4**, **6** and **9** were recorded and chemical shifts are given in Table 1. The spectra

Table 2 van der Waals volumes of ester residues and kinetic parameters for heterocyclic ring dynamics in **2**–**10**. Coalescence parameters are given in bold

Compounds	van der Waals volume of the ester residue/Å^3	T/K (°C)	τ/s	k/s^{-1}	$\Delta G^{\ddagger}$/ kJ mol^{-1}
2	26.89	297 (+24)	0.0049	204.1	
		294 (+21)	0.0063	158.5	
		293 (+20)	**0.0066**	**151.5**	**59.5**
		291 (+18)	0.0090	111.1	
		288 (+15)	0.012	83.3	
		283 (+10)	0.020	50.0	
3	43.65	293 (+20)	0.005	200.0	
		288 (+15)	**0.0073**	**137.0**	**58.6**
		283 (+10)	0.0105	95.5	
		278 (+5)	0.0295	33.9	
		273 (0)	0.055	18.2	
4	34.15	268 (−5)	0.0072	138.9	
		267 (−6)	**0.0072**	**137.2**	**54.2**
		263 (−10)	0.0118	84.7	
		260 (−13)	0.020	50.0	
		258 (−15)	0.025	40.0	
5	70.56	283 (+10)	0.0040	250	
		282 (+9)	**0.0054**	**185.2**	**56.7**
		281 (+8)	0.0078	128.2	
		278 (+5)	0.012	83.3	
6	76.89	318 (+45)	0.0025	400.0	
		315 (+42)	0.0037	270.3	
		312 (+39)	**0.0066**	**151.5**	**63.5**
		310 (+37)	0.008	125.0	
7	49.46	250 (−23)	0.04	25.0	
		255 (−18)	0.009	111.1	
		258 (−15)	**0.0054**	**185.2**	**51.65**
		260 (−13)	0.0040	250	
8	84.38	**307.5 (+34.5)**	**0.0085**	**117.6**	**63.2**
		305 (+32)	0.014	71.4	
		300 (+27)	0.022	83.3	
9	81.34	**303 (+30)**	**0.0072**	**138.9**	**61.8**
		302 (+29)	0.0072	137.9	
		293 (+20)	0.018	55.5	
		288 (+15)	0.045	22.2	
		283 (+10)	0.12	8.3	
10	128.95	223 (−50)	0.003	333.3	
		213 (−60)	0.0072	138.9	
		208 (−65)	**0.0073**	**137.0**	**41.8**

Table 3 The relevant results of GIAO CPHF calculations for **2**, **4**, **5** and **6**. Only one σ value is given when the difference in shielding constants for both orientations of the C=O group was smaller than 0.1 ppm

	Shielding, σ (ppm)			
	$OCOC(CH_3)_3$ (**6**)	$OCOCH_3$ (**2**)	$OCOCCl_3$ (**5**)	$OCOCF_3$ (**4**)
	C=O down (up)	C=O down (up)	C=O down (up)	C=O down (up)
O1	251.8 (252.6)	251.4 (251.7)	249.1 (249.5)	247.9 (248.2)
C2	138.27	138.17	138.02	137.76
C2b (axial)	176.46 (176.67)	176.48 (176.66)	176.47 (176.67)	176.33 (176.54)
C2a (equat.)	170.75	170.78	170.91	170.93
C3	170.75	170.83 (170.63)	171.00 (170.80)	170.94
C4	180.40	180.39	180.60	180.54
C5	73.00 (72.75)	72.43	71.95 (71.84)	71.97 (71.57)
C6	60.08 (60.19)	60.14	61.61 (61.77)	62.69
C7	69.71 (69.92)	70.14 (70.30)	68.92 (69.16)	69.51 (69.70)
C8	78.23 (78.15)	78.24 (78.19)	78.19 (77.95)	(77.60)
C8a	51.94	51.74 (51.59)	50.37	49.94 (49.79)
	[149.26][a]	[149.44]	[150.22]	[150.43]
C5a	187.33 (187.23)	187.51 (188.51)	187.20 (188.50)	187.74 (188.96)
C7a	187.23 (186.61)	187.35 (187.06)	187.09 (187.21)	186.99 (187.28)
O6a (ester)	158.8 (157.9)	151.8 (150.6)	159.4 (159.6)	157.5 (156.5)
C (carbonyl)	23.64 (24.10)	29.28 (29.61)	35.35 (35.68)	40.29 (40.86)
	[185.36]	[169.64]	[160.51]	[155.54]
O (carbonyl)	−79.5 (−78.6)	−96.3 (−95.1)	−107.3 (−107.9)	−101.4 (−99.7)

[a] Square brackets denote δ values.

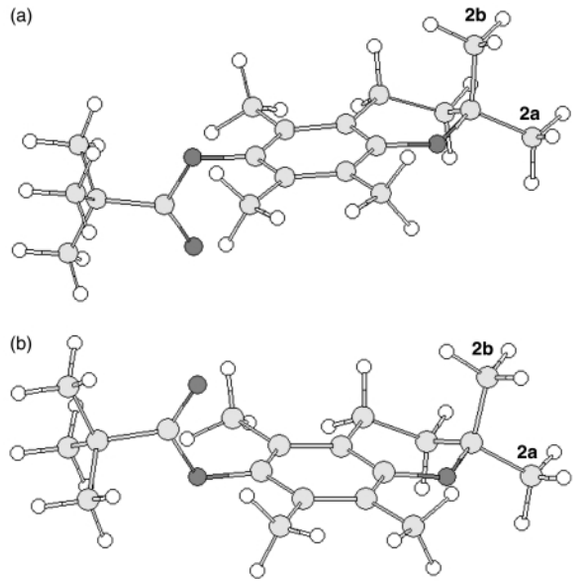

Fig. 3 The orientations of the ester substituent a) α (C=O downward), b) β (C=O upward).

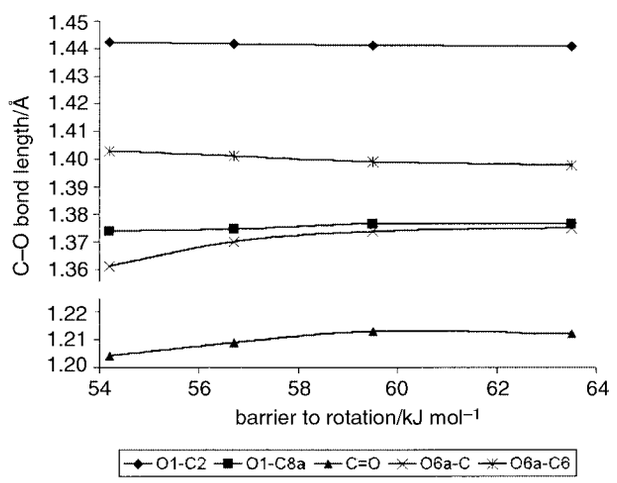

Fig. 4 Relationship between carbon–oxygen bond lengths and $\Delta G^{\ddagger}$ values for compounds **6**, **2**, **5** and **4**.

of compounds **2**, **3**, **4** and **9** are shown, as an illustration, in Fig. 5. In the spectra of **2**, **3** and **4**, the number of resonances is the same in solid as in solution. This shows that no polymorphism or pseudo-polymorphism occurs. The signals of aromatic carbons are narrow. The resonances of methylene carbons C3 and C4 are broader and suggest that some structural disorder within the saturated part of the ring appeared. The largest differences in chemical shifts between solution and the solid state are for *gem*-methyl carbons. Separate, sharp resonances of C2a and C2b confirm that there are no dynamics at C2 in the solids. The separation of methyl resonances is *ca*. 8 ppm for **1** and 5.5–6.7 ppm for the esters **2**, **3** and **4**. According to the X-ray diffraction (XRD) data[5] for **1**, there are two structurally different molecules in the unit cell. The main difference is in the conformation of the heterocyclic ring (torsion angle between the O1–C2 bond and the aromatic ring of 15.3 and 18.5 degrees and torsion angle between the C3–C4 bond and the aromatic ring of 11.6 and 10.7 degrees, respectively). There is no duplication of all resonances in the spectrum of solid **1**, although a remarkable peak splitting especially for C2, C3 and C4 could be expected. Nevertheless, the broad resonance of C4 and the splitting of C8 and C4a were observed.

^{13}C NMR solid state spectra of substituted *p*-hydroxybenzenes and methoxybenzenes were analysed by Saito *et al.*[17] They found that nonequivalence of electron density between carbons *ortho* to the hydroxy group is responsible for the splitting of resonances in ^{13}C NMR spectra. Frozen rotation around the C_{Ar}–O bond results in a deshielding of carbon proximate to the lone electron pair of oxygen whereas the shielding of carbon near the OH hydrogen is increased. The effect is most pronounced when the hydroxy group is coplanar with the aromatic ring. Similar changes of shielding were also observed for flavonoids and some polyphenols.[18] If the hydroxylic hydrogen in chroman-6-ol **1** is oriented toward C7, the deshielding of C5 and an increase of shielding at C7 would be observed (as compared with the values in solution). The changes of chemical shifts (Table 1) do not confirm the above prediction; the hydroxy group cannot be coplanar with the aromatic ring due to the presence of methyl groups at C5 and C7.

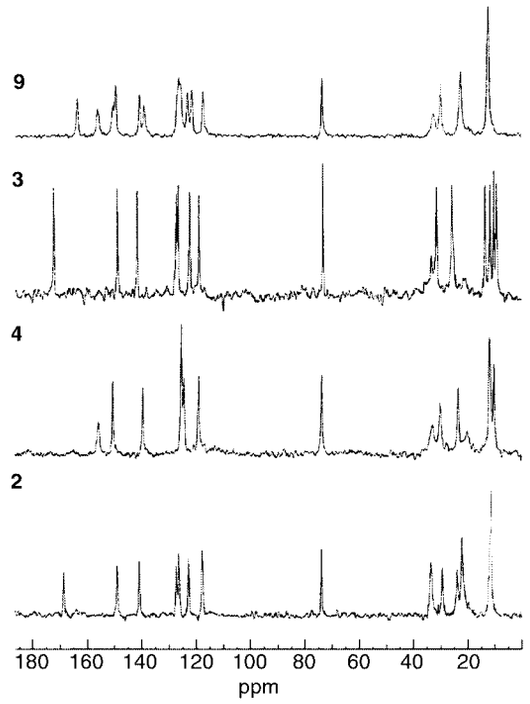

Fig. 5 ^{13}C CP MAS spectra of compounds **2**, **3**, **4** and **9**.

It is obvious that steric requirements of ester groups are larger than that for the hydroxy group and the ester substituents can be located either up (β) or down (α) from the plane of the aromatic ring. The fact that there are no significant differences between solution and solid state chemical shifts of C5, C7, C5a, C7a in esters of chromanol confirms the conformational rigidity of these molecules.

Experimental

IR spectra were measured on a Nicolette Magna 550 FTIR spectrometer for $CHCl_3$ solutions. ^{1}H and ^{13}C NMR spectra were recorded using a Bruker ACF spectrometer (200 MHz) equipped with a variable temperature probe for $CDCl_3$ solutions. Chemical shifts (δ) are downfield from TMS. Cross polarisation magic angle spinning (CP MAS) solid state ^{13}C NMR spectra were recorded on a Bruker MSL 300 instrument at 75.5 MHz. The samples were spun at 10 kHz; a contact time of 4 ms, a repetition time of 6 s, and a spectral width of 20 kHz for accumulation of 700–900 scans were used. Chemical shifts were calibrated indirectly through the glycine C=O signal recorded at 176.0 ppm relative to TMS.

The PM3 method implemented in the HyperChem package[15] was used in semi-empirical MO calculations. The calculations of shielding constants were performed on a Silicon Graphic Origin-200 workstation by the CPHF GIAO (6-31G**) methods from the GAUSSIAN 98 version.[16]

2,2,5,7,8-Pentamethylchroman-6-ol (**1**) (α-model compound) and 2,2,5,7,8-pentamethylchromane (**11**) (6-deoxy-α-model

Table 4 Melting points, IR, ^{1}H NMR and microanalytical data for compounds **1**–**11**

Compound	Mp/°C	IR (ν_{max}/cm^{-1})	^{1}H NMR (δ_H)	Elemental
1	92–94 (Lit.[19] 94–94.5)	2978, 2930, 1603, 1453, 1383, 1170, 1087, 923	4.23 (s, 1H, O*H*), 2.66 (t, *J* = 6.8 Hz, 2H, 4-H), 2.19 (s, 3H, ArC*H*$_3$), 2.15 (s, 6H, Ar (C*H*$_3$)$_2$), 1.82 (t, *J* = 6.9 Hz, 3-H), 1.32 (s, 6H, 2a and 2b-C*H*$_3$)	—
2	90–91.5 (Lit.[19] 92.5–93.5)	2979, 2930, 1745, 1454, 1369, 1168 and 1079	2.65 (t, *J* = 7.9 Hz, 2H, 4-H), 2.37 (s, 3H, C*H*$_3$CO), 2.13, 2.06 and 2.02 (3 × s, 9H, Ar (C*H*$_3$)$_3$), 1.82 (t, *J* = 7.8 Hz, 2H, 3-H), 1.34 (s, 6H, 2a and 2b-C*H*$_3$)	—
3	60–63	2981, 2943, 1747, 1461, 1416, 1164, 1125 and 1087	2.65 (m, 4H, 4-H and CH$_3$C*H*$_2$CO), 2.12, 2.04 and 2.00 (3 × s, 9H, Ar (C*H*$_3$)$_3$), 1.81 (t, *J* = 7.8 Hz, 2H, 3-H), 1.35 (t, *J* = 7.6 Hz, 3H, C*H*$_3$CH$_2$CO), 1.33 (s, 6H, 2a and 2b-C*H*$_3$)	Calcd for $C_{17}H_{24}O_3$: C, 73.88%; H, 8.75%. Found: C, 73.62%; H, 8.82%
4	63–66	2979, 2931, 1794, 1454, 1359, 1171, 1142 and 1108	2.65 (t, *J* = 7.7 Hz, 2H, 4-H), 2.14, 2.06 and 2.02 (3 × s, 9H, Ar (C*H*$_3$)$_3$), 1.94 (t, *J* = 7.7 Hz, 2H, 3-H), 1.34 (s, 6H, 2a and 2b-C*H*$_3$)	Calcd for $C_{16}H_{19}F_3O_3$: C, 60.75%; H, 6.05%. Found: C, 60.91%; H, 6.06%
5	126–130	2979, 2931, 1772, 1454, 1384, 1370, 1167, 1124, 1109 and 1064	2.65 (t, *J* = 6.7 Hz, 2H, 4-H), 1.83 (t, *J* = 6.2 Hz, 2H, 3-H), 2.14, 2.13 and 2.10 (3 × s, 9H, Ar (C*H*$_3$)$_3$), 1.34 (s, 6H, 2a and 2b-CH$_3$)	Calcd for $C_{16}H_{19}Cl_3O_3$: C, 52.55%; H, 5.24%. Found: C, 52.47%; H, 5.09%
6	78–81	2978, 2930, 1612, 1572, 1458, 1404, 1369, 1313, 1163, 1124, 1099, 970 and 923	2.62 (t, *J* = 6.9 Hz, 2H, 4-H), 2.08, 2.01 and 1.97 (3 × s, 9H, Ar (C*H*$_3$)$_3$), 1.79 (t, *J* = 6.9 Hz, 2H, 3-H), 1.41 (s, 9H, C(C*H*$_3$)$_3$), 1.30 (s, 6H, 2a and 2b-C*H*$_3$)	Calcd for $C_{19}H_{28}O_3$: C, 74.96%; H, 9.27%. Found: C, 75.03%; H, 9.42%
7	40–42 (Lit.[20] 50–52)	2981, 2932, 1752, 1460, 1370, 1166, 1123, 1095 and 1038	4.32 (q, *J* = 7.2 Hz, 2H, CH$_3$C*H*$_2$O), 2.62 (t, *J* = 6.8 Hz, 2H, 4-H), 2.11, 2.09 and 2.05 (3 × s, 9H, Ar (C*H*$_3$)$_3$), 1.80 (t, *J* = 6.8 Hz, 2H, 3-H), 1.40 (t, *J* = 7.2 Hz, 3H, C*H*$_3$CH$_2$O), 1.31 (s, 6H, 2a and 2b-C*H*$_3$)	Calcd for $C_{17}H_{24}O_4$: C, 69.84%; H, 8.27%. Found: C, 69.58%; H, 8.16%
8	154–156	2936, 1744, 1458, 1370, 1140, 1116 and 1079	8.3–7.47 (m, 5H, C$_6$*H*$_5$COO), 2.67 (t, *J* = 6.8 Hz, 2H, 4-H), 2.16, 2.10 and 2.06 (3 × s, 9H, Ar (C*H*$_3$)$_3$), 1.83 (t, *J* = 6.8 Hz, 2H, 3-H), 1.35 (s, 6H, 2a and 2b-C*H*$_3$)	Calcd for $C_{21}H_{24}O_3$: C, 77.75%; H, 7.46%. Found: C, 77.93%; H, 7.61%
9	136–137	2983, 2932, 1727, 1593, 1456, 1421, 1288, 1249, 1102 and 1025	9.46, 8.87, 8.49, 7.48 (4H, C$_5$*H*$_4$NCOO), 2.65 (t, *J* = 6.8 Hz, 2H, 4-H), 2.14, 2.07 and 2.03 (3 × s, 9H, Ar (C*H*$_3$)$_3$), 1.82 (t, *J* = 6.8 Hz, 2H, 3-H), 1.33 (s, 6H, 2a and 2b-C*H*$_3$)	Calcd for $C_{20}H_{23}NO_3$: C, 73.82%; H, 7.12%. Found: C, 74.02%; H, 7.27%
10	151–154	2980, 2930, 1599, 1460, 1369, 1263, 1124, 1108, 1059, 924 and 862	7.75 and 7.41 (dd$_{AB}$, *J* = 8.3 Hz, CH$_3$C$_6$*H*$_4$SO$_2$), 2.56 (t, *J* = 6.8 Hz, 2H, 4-H), 2.48 (s, 2H, C*H*$_3$C$_6$H$_4$), 2.05, 1.98, 1.94 (3 × s, 9H, Ar(C*H*$_3$)$_3$), 1.79 (t, *J* = 6.8 Hz, 2H, 3-H, 1.30 (s, 6H, 2a and 2b-C*H*$_3$)	Calcd for $C_{21}H_{26}SO_4$: C, 67.35%; H, 7.00%. Found: C, 67.54%; H, 7.22%
11	Oil (Lit.[19] 40–41)	2978, 2930, 1612, 1572, 1458, 1404, 1369, 1313, 1163, 1124, 1099, 970 and 923	2.61 (t, *J* = 6.9 Hz, 2H, 4-H), 2.21, 2.17 and 2.08 (3 × s, Ar(C*H*$_3$)$_3$), 1.80 (t, *J* = 6.9 Hz, 2H, 3-H), 1.32 (s, 6H, 2a and 2b-C*H*$_3$)	—

compound) were prepared as described by Smith *et al.*[19] 2,2,5,7,8-Pentamethylchroman-6-yl acetate (**2**), propionate (**3**), pivaloate (**6**), ethyl carbonate (**7**), benzoate (**8**) and nicotinate (**9**) were prepared according to a standard esterification method by means of the appropriate anhydride or acyl chloride in pyridine solution. Trifluoroacetate (**4**) was prepared by stirring compound **1** in trifluoroacetic anhydride at room temperature overnight. Trichloroacetate (**5**) was prepared following the procedures of Normant and Deshayes.[21] Tosylate (**10**) was prepared according to Miller and Wood.[22]

Acknowledgements

We thank Dr John D. Roberts (Professor Emeritus of California Institute of Technology) and the referees for valuable remarks.

References

1 P. B. McCay, K. L. Fong and M. M. King, in *Tocopherol, Oxygen and Biomembranes*, ed. C. deDuve and O. Hayashi, North-Holland and Biomedical Press, Amsterdam, 1978, pp. 41–57.
2 G. W. Burton and K. U. Ingold, *Acc. Chem. Res.*, 1986, **19**, 194.
3 I. H. Ekiel, L. Hughes, G. W. Burton, P. A. Jovall, K. U. Ingold and I. C. P. Smith, *Biochemistry*, 1988, **27**, 1432.
4 G. W. Burton, Y. Le Page, E. J. Gabe and K. U. Ingold, *J. Am. Chem. Soc.*, 1980, **102**, 7792.
5 K. Mukai, S. Obayashi, S. Nagaoka, T. Ozawa and N. Azuma, *Bull. Chem. Soc. Jpn.*, 1993, **66**, 3808.
6 G. W. Burton, T. Doba, E. J. Gabe, L. Hughes, F. L. Lee, L. Prasad and K. U. Ingold, *J. Am. Chem. Soc.*, 1985, **107**, 7053.
7 T. H. Siddal, W. E. Steward and M. L. Good, *Can. J. Chem.*, 1967, **45**, 1290.
8 I. Wawer, *Magn. Reson. Chem.*, 1988, **26**, 601.
9 M. Oki, in *Methods in Stereochemical Analysis*, vol. 4, VCH Publishers, Dearfield Beach, 1985, Chapter 7, pp. 287–304.
10 J. B. Lambert, C. E. Mixan and D. H. Johnson, *J. Am. Chem. Soc.*, 1973, **95**, 4634.
11 I. L. Shamovsky and I. Yu. Yarovskaya, *Chem. Pharm. J.*, 1990, **24**, 100.
12 I. L. Shamovsky, I. Yu. Yarovskaya, N. G. Khrapova and E. B. Burlakova, *J. Mol. Struct.* (*THEOCHEM*), 1992, **85**, 149.
13 J. J. P. Stewart, *J. Comput. Chem.*, 1989, **10**, 209.
14 J. J. P. Stewart, *J. Comput. Chem.*, 1989, **11**, 11, 211.
15 HyperChem 5.02, Hypercube Inc, Canada, 1997.
16 GAUSSIAN 98 Revision A.7, M. J. Frisch, G. W. Trucks, H. B. Schlegel, G. E. Scuseria, M. A. Robb, J. R. Cheeseman, V. G. Zakrzewski, J. A. Montgomery, Jr., R. E. Stratmann, J. C. Burant, S. Dapprich, J. M. Millam, A. D. Daniels, K. N. Kudin, M. C. Strain, O. Farkas, J. Tomasi, V. Barone, M. Cossi, R. Cammi, B. Mennucci, C. Pomelli, C. Adamo, S. Clifford, J. Ochterski, G. A. Petersson, P. Y. Ayala, Q. Cui, K. Morokuma, D. K. Malick, A. D. Rabuck, K. Raghavachari, J. B. Foresman, J. Cioslowski, J. V. Ortiz, A. G. Baboul, B. B. Stefanov, G. Liu, A. Liashenko, P. Piskorz, I. Komaromi, R. Gomperts, R. L. Martin, D. J. Fox, T. Keith, M. A. Al-Laham, C. Y. Peng, A. Nanayakkara, C. Gonzalez, M. Challacombe, P. M. W. Gill, B. Johnson, W. Chen, M. W. Wong, J. L. Andres, C. Gonzalez, M. Head-Gordon, E. S. Replogle and J. A. Pople, Gaussian, Inc., Pittsburgh, PA, 1998.
17 H. Saito, M. Yokoi, M. Aida, M. Kodama, T. Oda and Y. Sato, *Magn. Reson. Chem.*, 1988, **26**, 155.
18 I. Wawer and A. Zielinska, *Solid State NMR*, 1997, **10**, 33.
19 L. I. Smith, H. E. Ungnade, H. E. Hoehn and S. J. Wawzonek, *J. Org. Chem.*, 1939, **4**, 311.
20 L. I. Smith, W. B. Renfrow and J. W. Opie, *J. Am. Chem. Soc.*, 1942, **64**, 1084.
21 J. F. Normant and H. Deshayes, *Bull. Soc. Chim. Fr.*, 1972, 2854.
22 J. A. Miller and H. C. S. Wood, *J. Chem. Soc.* (*C*), 1968, 18.